Temperature dependence of the free volume from positron lifetime experiments and its relation to structural dynamics: Phenylphthalein-dimethylether

Günter Dlubek*
ITA Institute for Innovative Technologies, Köthen/Halle, Wiesenring 4, 06120 Lieskau, Germany

Muhammad Qasim Shaikh, Klaus Rätzke, and Franz Faupel
Faculty of Engineering, Christian-Albrechts University of Kiel, Kaiserstrasse 2, 24143 Kiel, Germany

Marian Paluch
Institute of Physics, Silesian University, Uniwersytecka 4, 40-007 Katowice, Poland
(Received 30 March 2008; revised manuscript received 19 September 2008; published 24 November 2008)

Positron annihilation lifetime spectroscopy (PALS) was used to study the microstructure of the free volume in the temperature range between 103 K and 393 K in phenylphthalein-dimethylether (PDE), a low-molecular-weight glass former. Using the routine LIFETIME9.0, the ortho-positronium (*o*-Ps) lifetime distribution was analyzed, and from this, the volume distribution $g_n(v_h)$ of subnanometer-size holes was calculated. From a comparison of PALS and specific volume data, the number density and the volume fraction of holes were estimated. These free-volume data, as a function of temperature, were used to test the validity of the Cohen-Turnbull (CT) free-volume theory. It was found that the structural relaxation from dielectric spectroscopy can be described by the CT theory after introducing a corrected free volume $(V_f - \Delta V)$, where $\Delta V = 0.014\ \mathrm{cm}^3/\mathrm{g}$. The extended free-volume theory of Cohen and Grest can be fitted to the dielectric-relaxation and free-volume data, but the parameters of both fits are not consistent. PDE shows some peculiar features. The "knee" in the *o*-Ps lifetime expansion and crossover in temperature dependence of the frequency of the primary dielectric relaxation process occur at different temperatures. In addition, the change in the Vogel-Fulcher-Tammann parameters at $T_B/T_g = 1.1$ has no observable effect on the mean free volume $\langle v_h \rangle$ (or V_f). The size of the smallest representative freely fluctuating subsystem, $\langle V_{SV} \rangle$ estimated from the standard deviation σ_h of $g_n(v_h)$, decreases from 4.1 nm^3 to 2.6 nm^3 when the temperature increases from $T/T_g = 1.0$ to 1.15. Correspondingly, the length of dynamic heterogeneity, $\xi = \langle V_{VS} \rangle^{1/3}$, decreases from 1.6 nm to 1.4 nm. It is concluded that at $T/T_g \approx 1.10 = T_B/T_g$ the system transforms from a heterogeneous to a homogeneous (true) liquid.

DOI: 10.1103/PhysRevE.78.051505 PACS number(s): 64.70.P−, 65.20.−w, 61.20.−p, 78.70.Bj

I. INTRODUCTION

The fundamental mechanisms underlying the glass transition of a glass-forming liquid continue to be studied and are strongly debated [1–13]. In this field, some common aspects in the dynamics of different systems suggest that, despite material-specific aspects, some common description should also be possible. For instant, low-molecular-weight liquids and polymeric melts show similar behavior of the primary (α-) relaxation dynamics, which is directly related to the liquid-glass transition. As the temperature is reduced, the molecular motions in a liquid become more restricted, due to both the decrease of thermal energy and the increased molecular crowding. Thus the properties near T_g mirror both thermal and volume effects.

Only limited experimental information about the free volume and its (thermal or frozen) spatial fluctuations are available. During the past decade positron annihilation lifetime spectroscopy (PALS) has developed to be the most important experimental method for studying subnanometer-size holes in polymers and low-molecular-weight organic materials [14–19]. In molecular solids and liquids a fraction of the positrons injected from a radioactive source form positronium (Ps), a light quantum-mechanical particle with the mass of two electrons and the size of a hydrogen atom. A positron can annihilate via one of the three decay channels—that is, as *para*-Ps (*p*-Ps, singlet state, channel 1, mean lifetime $\tau_1 \approx 0.12$ ns), positrons having not formed Ps (e^+, channel 2, $\tau_2 \approx 0.3$ ns), and *ortho*-Ps (*o*-Ps, triplet state, channel 3, $\tau_3 = 0.5 - 10$ ns).

In amorphous materials Ps is *Anderson* localized in a subnanometer-size hole of the free volume [20,21]. The long-lived *o*-Ps is very sensitive to the hole size. Its lifetime decreases from 142 ns in infinitely large holes (self-annihilation in a vacuum) to the low ns range in subnanometer-size holes and reflects the hole size (and shape) at the moment of annihilation [22–24]. The decrease in lifetime occurs, as *o*-Ps may annihilate with an electron other than its bound partner and with opposite spin, during a collision with a molecule in the hole wall (pickoff annihilation). Due to the Anderson localization, the *o*-Ps will not leave the hole where it is formed or first trapped. Therefore, the *o*-Ps lifetime shows a distribution which comes from the size (and shape) distribution of holes [25,26]. In studies of small molecule substances, this fact is frequently ignored.

PALS itself is suited to measure the mean volume of the holes and, with larger limitations, their size distribution. It is, however, impossible to directly measure the hole density or the hole fraction. It was shown that a correlation of PALS

*Author to whom correspondence should be addressed. guenter.dlubek@gmx.de

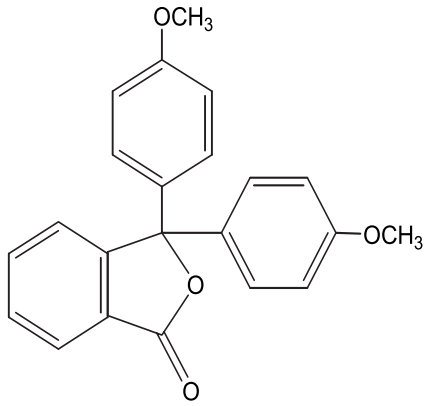

FIG. 1. Chemical structure of PDE.

results with macroscopic volume data can provide an estimate of the specific (*o*-Ps) hole density [27,28].

In previous works some of us have measured the hole volume in various polymers by PALS and compared the experiments with gas diffusion data [19,29] and with theoretical hole size distributions from molecular dynamics simulations [30,31]. Also some of us have determined the hole size distribution and calculated the hole density and hole fraction from a comparison of PALS results with those from the S-S equation-of-state (EOS) analysis of pressure-volume-temperature (PVT) experiments. These data were used to test the validity of the free-volume theory for the diffusion of ions [32,33] and the segmental relaxation in polymers [34–39] to derive free-volume fluctuations and to discuss them in relation to the heterogeneity of polymer dynamics [39,40].

In this work we study the free volume in phenylphthalein-dimethylether (PDE), a low-molecular-weight (M_w=346 g/mol) glass former which shows structural dynamics comparable to polymers [9–11]. The chemical structure of PDE is shown in Fig. 1. Our chief motivation is to characterize the free-volume structure as completely as possible and use it to test the validity of the classical Cohen-Turnbull (CT) free-volume theory [12] for the structural relaxations. Furthermore, we also fit the free-volume model of Cohen and Grest (CG) [13] to the structural-relaxation and free-volume data and check the mutual consistency of the parameters obtained herewith.

Small molecule glass formers have been already studied by several groups, and the PALS data were correlated to viscosity, dielectric relaxation, and incoherent elastic neutron-scattering measurements [15,16,37,41–49]. We go beyond these previous works by calculating from our positron lifetime spectra the hole size distribution characterized by its mean and width. Accordingly we employ the routine LIFETIME, version 9.0 (LT9.0) [50]. From the width of the hole size distribution the length of scale of dynamic heterogeneity can be estimated employing a fluctuation approach [40]. Furthermore, we estimate the hole density and the hole fraction from a correlation of PALS with PVT data. To our best knowledge, PDE was not yet studied by PALS.

A detailed investigation of the dynamics of this material employing dynamic light-scattering-photon correlation-spectroscopy (DLS-PCS) was recently published by Patkowski *et al.* and one of us [9–11]. They also presented PVT experiments of PDE [10]. In the present work we use these data and the dielectric-relaxation times by Stickel *et al.* [51] for a comparison with our PALS experiments.

II. EXPERIMENT

The PDE sample for PALS measurements was prepared from the same material investigated in the past by DLS-PCS and PVT experiments [9–11]. It was synthesized in the laboratory of Professor H. Sillescu at Johannes Gutenberg University, Mainz, Germany. PVT experiments delivered a glass transition temperature T_g=298 K and a melting temperature T_m=373 K [10]. The T_g corresponds to a temperature (296 K) where the relaxation time from DLS-PCS experiments is equal to 10^2 s [9].

Positron annihilation lifetime experiments have been performed with a fast-fast coincidence setup [15] using a homemade temperature-controllable sample holder under high-vacuum conditions as described in more detail in a recent work [29]. The time resolution was 285 ps [full width at half maximum (FWHM), ^{22}Na source], and the analyzer channel width amounted to 25.3 ps. PDE available in the form of crystalline powder was sandwiched around a ~1-MBq positron source ^{22}NaCl, deposited between two 7-μm-thick Kapton foils. It was first measured at room temperature, then heated in the sample holder to 393 K for melting and measured at this temperature. Subsequently, the sample was cooled to 103 K and the temperature run was started. This treatment undercools the melt and transforms PDE at low temperatures into an amorphous, glassy state. During the experiments the temperature was increased between 103 K and 393 K in steps of 10 K (accuracy of $\pm$2 K). Source correction, 8.4% of 395 ps (Kapton foil and ^{22}NaCl), and time resolution were determined by measuring a defect-free *p*-type silicon reference (τ=219 ps). The final resolution function used in the spectrum analysis was determined as a sum of two Gaussian curves. Each measurement lasted 2 h, leading to a lifetime spectrum with the high number of $\sim 5 \times 10^6$ annihilation events, which is sufficiently high to be analyzed with the routine LT9.0 in its distribution mode.

III. RESULTS AND DISCUSSION

A. Spectrum analysis and lifetime parameters

The positron lifetime spectrum $s(t)$ is given by the Laplace transformation of the sum of the functions $\alpha_i(\lambda)\lambda$, $s(t)=\Sigma I_i \int \alpha_i(\lambda)\lambda \exp(-\lambda t)d\lambda$, where $\alpha_i(\lambda)$ is the distribution [probability density function (PDF)] of the annihilation rate $\lambda=1/\tau$ of the decay channel i [25,26]. As already mentioned, the positron decay in molecular solids and liquids shows usually three decay channels which are attributed to the annihilation of *p*-Ps (τ_1), free (not Ps) positrons (e^+, τ_2), and *o*-Ps (τ_3; $\tau_1 < \tau_2 < \tau_3$) [14–19]. The conventional lifetime analysis (routine PATFIT [52], for example, or LT9.0 in the discrete-term mode) assumes that each $\alpha_i(\lambda)$ follows a δ function which leads to a sum of three discrete exponential functions for $s(t)$, $s(t)=\Sigma(I_i/\tau_i)\exp(-t/\tau_i)=\Sigma(I_i\lambda_i)\exp(-\lambda_i t)$, where their relative intensities follow: $I_1+I_2+I_3=1$. The lifetime spectra show, however, a nonexponential behavior

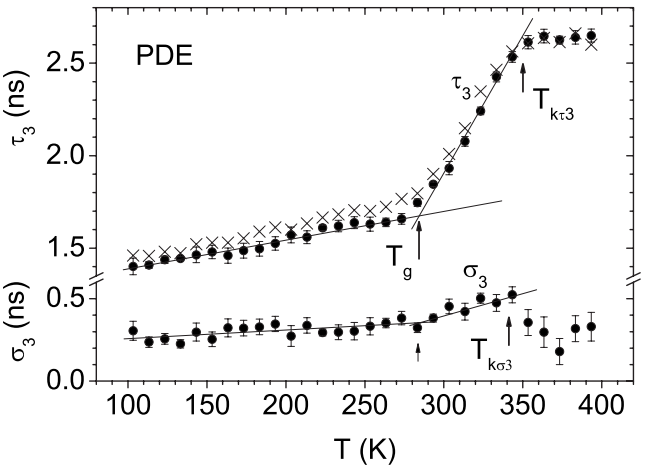

FIG. 2. Mean, $\tau_3 \equiv \langle \tau_3 \rangle$, and standard deviation, σ_3, of the *o*-Ps lifetime distribution in PDE. T_g indicates the glass transition temperature and $T_{k\tau 3}$ and $T_{k\sigma 3}$ the "knee" temperature for τ_3 and σ_3. The lines through the data points are a visual aid. The crosses show, for comparison, the τ_3 values from an unconstrained three-exponential-(discrete) term fit.

[25,26]. The least-squares routine LT9.0 [50] takes this into account by assuming that the functions $\alpha_i(\lambda)$ follow a log-normal distribution. This assumption comes from many years experience with the routine CONTIN, a numerical Laplace inversion technique [25]. The lifetime spectrum is expressed by

$$s(t) = I_1 \lambda_1 \exp(-\lambda_1 t) + \sum_{i=2,3} I_i \int_0^\infty \alpha_i(\lambda) \lambda \exp(-\lambda t) d\lambda, \tag{1a}$$

with

$$\alpha_i(\lambda) \lambda d\lambda = \frac{1}{\sigma_i^* (2\pi)^{1/2}} \exp\left(- \frac{(\ln \lambda / \lambda_{i0})^2}{2\sigma_i^{*2}} \right) d\lambda, \tag{1b}$$

where $\int \alpha_i(\lambda) d\lambda = 1$ and $\Sigma I_i = 1 (i = 1,2,3)$. The routine LT9.0 delivers as output not the parameters of the annihilation rate distribution, λ_{i0} and σ_i^*, but the mean lifetime $\tau_i \equiv \langle \tau_i \rangle$ and the standard deviation (root-mean-square deviation) σ_i of the corresponding lifetime distribution $\alpha_i(\tau) = \alpha_i(\lambda) d\lambda / d\tau = \alpha_i(\lambda) \lambda^2$ $(\tau = 1/\lambda)$ together with the intensities I_2 and I_3 $(I_1 = 1 - I_2 - I_3)$. $\tau_i \equiv \langle \tau_i \rangle$ and σ_i are defined as the first momentum $(\langle \tau_i \rangle = \int \tau \alpha_i(\tau) d\tau)$ and the square root of the second momentum [the variance $\sigma_i^2 = \int (\tau - \langle \tau_i \rangle)^2 \alpha_i(\tau) d\tau$] of the lifetime τ. The relations between the parameters of both distributions, $\alpha_i(\tau)$ and $\alpha_i(\lambda)$, are $\langle \tau_i \rangle = [\exp(\sigma_i^{*2}/2)]/\lambda_{i0}$ and $\sigma_i = \tau_i [\exp(\sigma_i^{*2}) - 1]^{0.5}$ [50]. In order to reduce the number of fitting parameters we assumed, as usual, that the lifetime spectrum of the fast decaying *p*-Ps $(i=1)$ is described by a discrete exponential function $(\sigma_1 = 0)$ and fixed the *p*-Ps intensity I_1 to the theoretical *p*-Ps/*o*-Ps formation ratio of $I_1/I_3 = 1/3$ [14–16]. The reduced χ^2 of the fits, χ^2/df, were usually better than 1.05, showing the high quality of the fit.

Figure 2 shows the temperature dependence of the mean and standard deviation of the lifetime distribution of *o*-Ps, τ_3, and σ_3. For comparison, the τ_3 parameter determined from the conventional analysis assuming three (unconstrained) discrete exponential lifetime terms is also depicted in Fig. 2. The τ_3 values obtained from this fit are only slightly larger (due to the ignorance of the distribution) than the *o*-Ps lifetimes determined from the more advanced distribution analysis. The *o*-Ps intensity I_3 (not plotted) shows between 100 K and 280 K (a temperature near T_g) an increase from 8.0% to 11.2(±0.2)% followed by a slight decrease to 9.7% at 390 K. I_3 has no simple relation to the free volume, but mirrors the complex kinetics of *o*-Ps formation (see [15,17,53]), so we move on without further discussion of this parameter.

The *o*-Ps lifetime parameters τ_3 and σ_3 mirror the thermal expansion of the holes where *o*-Ps is localized and annihilated, its mean size and width of the hole size distribution. They show the expected behavior: a weak linear increase below T_g and a steeper increase above that temperature. σ_3 follows the behavior of τ_3 and can be fitted by $\sigma_3 = 0.283(\pm 0.006)(\tau_3 - 0.5)$ (all data from below $T_{k\sigma 3}$) where 0.5 ns is the limit of the *o*-Ps lifetime for disappearing hole size. At higher temperatures the increase of both parameters levels off. Since this temperature denoted as the "knee" temperature may differ for the parameters τ_3 and σ_3, we describe these points as $T_{k\tau 3}$ and $T_{k\sigma 3}$. Above the "knee" temperature the *o*-Ps lifetime no longer correctly mirrors the hole size (see the discussion in a subsequent part).

The behavior of τ_3 and σ_3 for PDE corresponds closely to that observed for other molecular materials, such as monomeric and oligomeric (uncured) epoxy resin diglycidyl ether of bisphenol-A (DGEBA) [37,38] and polymers with flexible chains, like polymethylphenylsiloxane (PMPS) [39] and polyisobutylene (PIB) [35]. In polymers with stiff chains (and high T_g), τ_3 and particularly σ_3 may exhibit distinctly larger values [54].

We remark at this point that the crystalline PDE powder measured at 300 K before melting even shows Ps formation with *o*-Ps lifetime parameters of $\tau_3 = 1.07$ ns and $\sigma_3 = 0.35$ ns. This result indicates that the PDE crystallites contain vacancy-type defects, however, of a size smaller than a gap between the molecules in the supercooled liquid at the same temperature [55]. It can not be excluded, however, that Ps is formed at interstitial sites of crystals, as observed for polyethylene and tetrafluoroethylene [56].

The *p*-Ps lifetime τ_1 (not displayed) shows a slight increase with temperature from 0.163 ns to 0.177(±0.005) ns. Fixing of τ_1 to the lifetime of *p*-Ps in a vacuum, 0.125 ns, did not change the lifetime parameters, except a slight increase of σ_2 by 0.007 ns and σ_3 by 0.05 ns. The lifetime parameters τ_2 and σ_2 of positrons having not formed Ps (e^+) exhibit a behavior almost parallel to the corresponding *o*-Ps lifetime parameters: a distinct change in the slope at the glass transition temperature, however, with the clear exception that a leveling off does not occur (not shown). Linear least-squares fits delivered (all parameters in ns)

$$\tau_2 = 0.229(\pm 0.001) + 0.0144(\pm 0.0006)(\tau_3 - 0.5) \tag{2}$$

and

$$\sigma_2 = -0.281(\pm 0.01) + 1.58(\pm 0.06)\tau_2. \tag{3}$$

B. Temperature dependence of hole size

In the following section we calculate the hole volume distribution from the *o*-Ps annihilation rate distribution and discuss the temperature dependence of the mean and width of this distribution. Based on the semiempirical standard model [22] the *o*-Ps pickoff annihilation rate λ_{po}, the inverse of the *o*-Ps lifetime $\tau_{po}=\tau_3$, is related to the hole (assumed spherical) radius (r_h) via

$$\lambda_{po}=1/\tau_{po}=2\ \mathrm{ns}^{-1}\left[1-\frac{r_h}{r_h+\delta r}+\frac{1}{2\pi}\sin\left(\frac{2\pi r_h}{r_h+\delta r}\right)\right], \tag{4}$$

where $\delta r=1.66$ Å [23,24] describes the penetration of the Ps wave function into the hole walls. The mean hole volume is usually calculated from $v_h(\tau_3)=(4/3)\pi r_h^3(\tau_3)$. Since λ_{po} follows a distribution, we have estimated, as in our previous works [34–39], the mean hole volume as the mass center of the hole size distribution. The radius distribution $n(r_h)$ can be calculated from $n(r_h)=-\alpha_3(\lambda)d\lambda/dr_h$ [25,26], where $\alpha_3(\lambda)$ is the *o*-Ps annihilation rate distribution calculated from the parameters of the LT analysis. The hole volume distribution follows from $g(v_h)=n(r_h)/4\pi r_h^2$.

It is not completely clear whether *o*-Ps samples holes of different size with the same probability. Frequently an increasing weight with increasing hole size is assumed [57]. Following this line we assume in our works that $n(r_h)$ and $g(v_h)$ represent volume-weighted functions [34–39]. Then the number-weighted hole size distribution follows from $g_n(v_h)=g(v_h)/v_h$. We have calculated the mean $\langle v_h\rangle$ and the variance σ_h^2 of $g_n(v_h)$ as first and second moments of this distribution. For comparison, in this work we also calculated the mean and variance of $g(v_h)$, denoted as $\langle v_h\rangle_v$ and σ_{hv}^2.

The mean and standard deviation of the hole volume distribution are plotted in Fig. 3. The parameters $\langle v_h\rangle$ and σ_h as well as $\langle v_h\rangle_v$ and σ_{hv} show the expected behavior. At the glass transition the thermal expansivity, $e_h=d\langle v_h\rangle/dT$, and the coefficient of thermal expansion, $\alpha_h=e_h/\langle v_{hg}\rangle$ ($\langle v_{hg}\rangle=\langle v_h(T_g)\rangle$), of free-volume holes change abruptly for values from the glass to the rubber. The parameters T_g, T_0', $\langle v_{hg}\rangle$, σ_{hg}, e_h, and α_h listed in Table I were obtained from linear fits (Fig. 3). T_0' is the temperature where the hole volume linearly extrapolated from the state above T_g vanishes.

Below T_g, *o*-Ps is trapped in a local free volume within the glassy matrix, and the *o*-Ps lifetime and the calculated hole size mirror the mean size of more or less static holes. In the region $T>T_g$ the structural mobility increases rapidly in frequency [9,51] and amplitude [58], which leads to a steep rise in $\langle v_h\rangle$ and σ_h with the temperature. The mean-hole-size dispersion σ_h shows a similar glass transition behavior as $\langle v_h\rangle$. At a temperature of $T_{kv}=T_k\langle v_h\rangle=T_g+68\ \mathrm{K}=360\pm5$ K (the $\langle v_h\rangle$ "knee," $T_{kv}/T_g=1.23$) the mean hole volume $\langle v_h\rangle$ levels off. For polymers this effect has been attributed to structural (segmental) motions; their mean relaxation time τ_α reaches at T_{kv}, the order of magnitude of τ_3 [33–47]. Similar interpretations were published for small-molecule glass formers [16,47,49]. As long as the τ_α is significantly larger than the mean lifetime τ_3, *o*-Ps provides "snapshots" of the free-volume microstructure at the moment of annihilation.

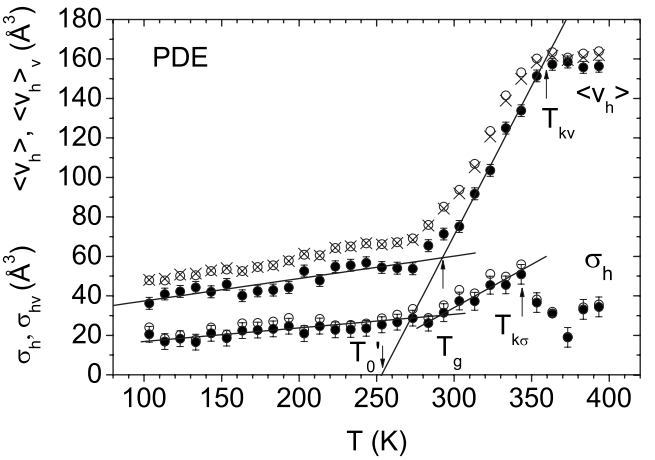

FIG. 3. The temperature dependence of the hole volume of PDE. Shown are the mean and the standard deviation of the function $g_n(v_h)$, $\langle v_h\rangle$, and σ_h (solid symbols) and of the function $g(v_h)$, $\langle v_h\rangle_v$, and σ_{hv} (open symbols). The crosses show the hole volume calculated directly from the mean *o*-Ps lifetime, $\tau_3\equiv\langle\tau_3\rangle$, via $v_h(\tau_3)=4\pi r_h^3/3$. The lines through $\langle v_h\rangle$ are linear fits to the data from the temperature regions between 103 and 273 K and 303 and 353 K while the lines through σ_h are a guide for the eyes.

Hence, τ_3 and σ_3 mirror the fluctuations of holes sizes and shapes in space and time like a quasistatic hole size distribution. For structural relaxation times of the order of τ_3, the hole walls are likely to move during the lifetime of *o*-Ps, which effectively reduces the empty space inside the holes probed by *o*-Ps.

From the dielectric spectroscopy data of Stickel *et al.* [51] we found that a structural (α-)relaxation time $\tau_\alpha=1/\nu_\alpha$ is equal to 63 ns at 360 K. This value is larger by a factor of $\approx$30 than the *o*-Ps lifetime τ_3. Possibly, intramolecular relaxations such as phenyl ring flip and reorientation of the —OCH_3 group [59] may cause this effect. Note that the appearance of the PALS "knee" (T_{kv}) at an unexpectedly

TABLE I. Results from the analysis of the PALS experiments (for explanation of symbols, see the text). The parameters were calculated from linear fits to the experimental data from the ranges between 100 and 270 K and 300 and 350 K.

Quantity	Uncertainty	From $\langle v_h\rangle_v$	From $\langle v_h\rangle$
T_g (K)	±3	285	292
T_0' (K)	±10	236	253
$\langle v_{hg}\rangle$ (Å^3)	±3	70.8	58.4
σ_{hg} (Å^3)	±2	30	28
e_{hg} (Å^3/K)[b]	±0.02	0.13	0.11
e_{hr} (Å^3/K)[c]	±0.05	1.43	1.51
α_{hg} (10^{-3} K^{-1})[b]	±0.2	1.87	1.84
α_{hr} (10^{-3} K^{-1})[c]	±1	20.2	25.9
N_h' (10^{21} g^{-1})	±0.02	0.332	0.321
N_h (nm^{-3})[a]	±0.02	0.46	0.44

[a]At 300 K.
[b]At $T\to T_g$. $T<T_g$.
[c]At $T\to T_g$, $T>T_g$.

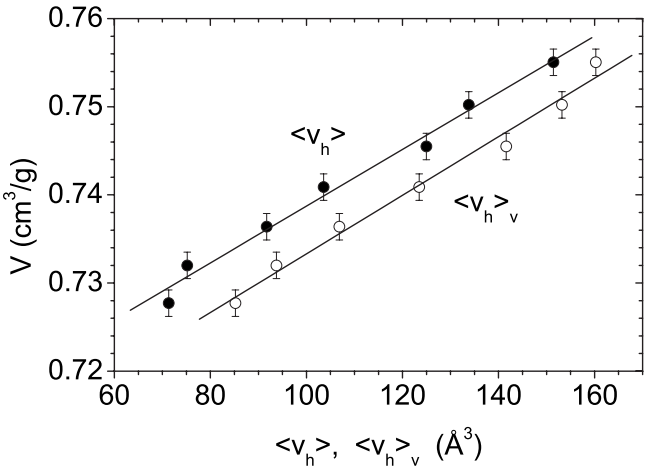

FIG. 4. The specific volume $V(T)$ of PDE for the temperature range between 293 K and 353 K plotted vs the mean hole volumes $\langle v_h(T)\rangle$ (solid circles) and $\langle v_h(T)\rangle_v$ (open circles), respectively. The lines are linear fits to the data.

large value of $\tau_\alpha \approx 10^{-6}$ s was also discussed by Ngai *et al.* [44] for several other small-molecule glass formers. It was observed, however, that T_{kv} correlates well with incoherent elastic neutron-scattering measurements of the mean-square atomic displacement $\langle u^2\rangle$, which shows for fast motions of $\geqslant 10^8$ Hz a strong nonlinear increase above T_{kv} (labeled as T_r or T_{b2}). This was explained by arguing that both τ_3 and $\langle u^2\rangle$ reflect the level of anharmonicity in motions of molecules caged in an unoccupied volume defined by its nearest neighbors [44].

C. Density of holes

The mean specific hole density N_h' can be estimated from a comparison of PALS data with the macroscopic volume using the relation [27,28]

$$V = V_{\mathrm{occ}} + N_h' \langle v_h \rangle, \tag{5}$$

where V, V_{occ}, and $V_f = N_h' \langle v_h \rangle$ are the specific total, occupied, and free volumes. Figure 4 shows the specific volume $V(T)$ plotted against both types of hole volume, $\langle v_h(T)\rangle$ and $\langle v_h(T)\rangle_v$, in the temperature range between T_g and T_{kv}. $V(T)$ was calculated from the parameters of the Tait equation fitted to the PVT data of PDE by one of us [10], which gave for $T > T_g$

$$V(T) = 0.718(\pm 0.004) + 0.4100(\pm 0.002) \times 10^{-3} T + 5.0714(\pm 0.095) 10^{-7} T^2, \tag{6}$$

where V and T are given in cm^3/g and °C, respectively. As observed in Fig. 4 both data sets show a linear correlation. Assuming that V_{occ} does not change with temperature, the slope of the respective data sets seems to indicate a constant specific hole density.

A very qualified method for the estimation of the free volume is established by the S-S EOS [60–62]. This statistical mechanics theory describes the disordered structure of a liquid by a lattice with a fraction of occupied cells of less than 1. An analysis of the PVT data of melts employing this theory delivers explicitly the fraction h of holes (vacancies of the S-S lattice) and its specific volume $V_f = hV$. Several groups [28,63–66] and also some of us [32,34–39,67,68] have applied this analysis in comparison with PALS studies for various polymers. It is well known that above T_g the occupied volume V_{occ} is almost constant. Below T_g, V_{occ} expands with approximately half of the glass expansion coefficient. The hole density derived from the $V_f = hV$ vs $\langle v_h\rangle$ plot is constant and does not change at the glass transition. Unfortunately, for the S-S EOS one needs information on the external (volume-dependent) degrees of freedom number, as well as on the number of intermolecular contacts, as input of the calculation. The calculations are well defined only for simple molecules such as spherical or linear molecules [60–62]. A more complex shape of molecules makes its application complicated, and the calculations are not well theoretically based [69].

However, it was found that for the liquid state the hole density derived from the $V_f = hV$ vs $\langle v_h\rangle$ plots agrees with the slope of the V vs $\langle v_h\rangle$ dependences and the fitted V_{occ} agrees with that calculated from the S-S EOS [28,33–39]. Therefore, the hole density may be easily calculated from the plots shown in Fig. 4, assuming the constancy of V_{occ} and of the hole density [27]. We obtained from a linear fit to the V vs $\langle v_h\rangle$ plot the parameters

$$V_{\mathrm{occ}} = 0.7066(\pm 0.002)\ \mathrm{cm}^3/\mathrm{g}$$

and

$$N_h' = dV/d\langle v_h\rangle = (dV/dT)/(d\langle v_h\rangle/dT) = 0.321(\pm 0.02) 10^{21}\ \mathrm{g}^{-1}.$$

Assuming that $\langle v_h\rangle_v$ is not a volume-weighted value, but a number-weighted value, the fit to the V vs $\langle v_h\rangle_v$ plot delivers $V_{\mathrm{occ}} = 0.7000(\pm 0.002)\ \mathrm{cm}^3/\mathrm{g}$ and $N_h' = dV/d\langle v_h\rangle_v = (dV/dT)/(d\langle v_h\rangle_v/dT) = 0.332(\pm 0.02) 10^{21}\ \mathrm{g}^{-1}$. The specific hole densities correspond to the volume related hole densities, $N_h = N_h'/V$, of 0.44 nm^{-3} and 0.46 nm^{-3} at a temperature of 300 K [$V(300) = 0.7294\ \mathrm{cm}^3/\mathrm{g}$]. These hole densities are in the range of those found for polymers (0.3–0.9 nm^{-3}) [34–39,63,64] and monomeric DGEBA (0.65 nm^{-3}) [37].

Using the known hole density for PDE and the assumption that it does not change with the temperature, we may calculate the specific free volume $V_f(T) = N_h' \langle v_h\rangle$ for the glass and the liquid. These data are shown in Fig. 5 together with V_f calculated from the relation $V_f = V - V_{\mathrm{occ}}$, where V_{occ} was assumed to be constant in the whole temperature range above T_g and was taken from the plots in Fig. 4 ($V_{\mathrm{occ}} = 0.7066\ \mathrm{cm}^3/\mathrm{g}$). For clarity, we have shown in Fig. 5 only the values derived from the parameters $\langle v_h\rangle$ and σ_h. The volumes calculated from $\langle v_h\rangle_v$ and σ_{hv} differ somewhat from the former ones, but the conclusions do not change.

The plot shows the glass transition and the leveling off of the PALS data at the knee temperature T_{kv} ($\approx T_{k\tau 3}$). It is expected that the true free volume increases in a continuous manner above this temperature in its almost linear expansion as shown by $V_f = V - V_{\mathrm{occ}}$. The fractional free volume can now be calculated from $f = V_f/V$. Both parameters can be

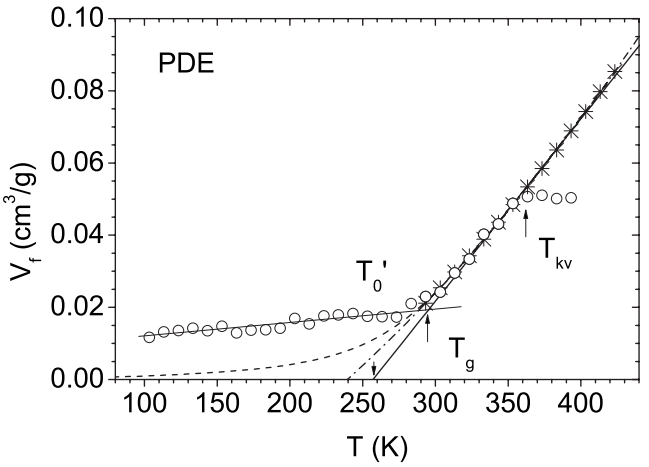

FIG. 5. Specific free volume calculated from PALS, $V_f = N_h' \langle v_h \rangle$ (open circles), and PVT data, $V_f = V - V_{occ}$ where $V_{occ} = 0.7066$ cm^3/g (stars). The lines show the following fits: solid line, linear fit to $V_f = V - V_{occ}$ in the temperature range 333 K $< T <$ 403 K; dashed-dotted line, quadratic fit; dashed line, fit of the Cohen-Grest equation (see a later section), both in the range 293 K $< T <$ 423 K.

best fitted by a second-order polynomial with the parameters $a_0 = -0.055\,04$, $a_1 = 0.972 \times 10^{-4}$, and $a_2 = 5.54 \times 10^{-7}$ for V_f (given in cm^3/g) and $b_0 = -0.1122$, $b_1 = 3.95 \times 10^{-4}$, and $b_2 = 2.96 \times 10^{-7}$ for f (T in K). The specific hole free volume V_f varies (in the range from $T_g = 292$ K to 423 K) from $V_f = 0.0206$ to 0.0854 cm^3/g, and the free-volume fraction f varies from $f = 0.0283$ to 0.1078. The small value of f_g (=0.0283) shows the dense packing of the glassy PDE and corresponds to those estimated for polymers with flexible chains ($f_g = 0.0150$ at $T_g = 210$ K for PIB [43] and $f_g = 0.0343$ at $T_g = 260$ K for PMPS [39], as examples), while polymers with stiff chains may show values up to $f_g = 0.305$ ($T_g = 510$ K, Teflon AF2400) [54]. The quadratically extrapolated volume $V_f = V - V_{occ}$ vanishes at 240 K. An alternative linear fit to the V_f data from the temperature range between 333 and 403 K delivers $T_0' = = 257$ K (see Fig. 5). The fits of the CG model [13] to the volume data we will discuss in a later section.

D. Free volume and structural dynamics

In the following section we attempt to analyze the dynamic properties of PDE as shown by dynamic light scattering (DLS-PCS) and dielectric spectroscopy (DS) in terms of the CT free-volume model [12]. We will focus on the DS data of Stickel *et al.* [51], which agree with the DLS-PCS results of Patkowski *et al.* [9], but extend to distinctly larger frequencies. The bottom part of Fig. 6 shows the relaxation map of PDE in the form of the classical Arrhenius plot: i.e., the plot of the peak frequency $\nu(\mathrm{Hz}) = \nu_{max}$ of the dielectric loss function ε'' attributed to the primary (α-)relaxation process versus inverse of temperature.

The dynamics of structural relaxation is usually described by the Vogel-Fulcher-Tammann (VFT) law [51]

$$\nu = \nu_0 \exp[-B/(T - T_0)], \tag{7}$$

where B and T_0 are assumed to be constant. Stickel *et al.* [51] found that Eq. (7) fits the frequency data of PDE in the

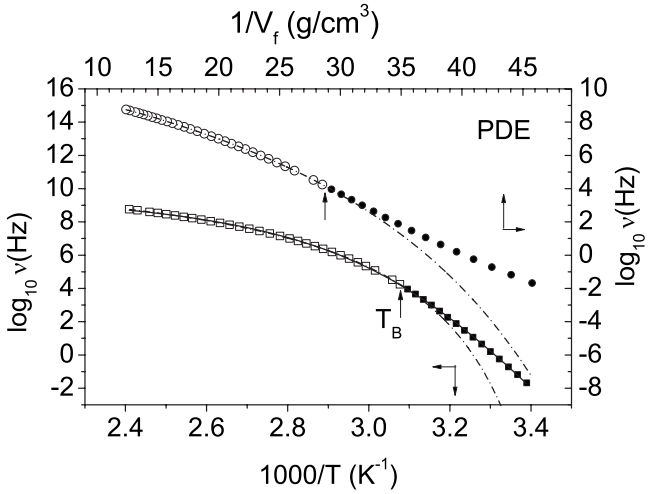

FIG. 6. Arrhenius plot (squares, bottom x and left y axes) and Cohen-Turnbull plot (circles, top x and right y axes) of the peak frequency ν of dielectric loss ε'' of the main relaxation process in PDE. The frequency data are from Stickel *et al.* [51] and cover a temperature range between 295 K and 415 K. The dashed-dotted lines are VFT and CT fits to the data in the temperature range between $T_B = 325$ K and 415 K (open symbols). The solid line of the bottom plot shows a fit of the Cohen-Grest model to the data from the entire temperature range.

temperature range from a lower boundary of $T_B = 325$ K and the maximum measuring temperature of 415 K. These authors also pointed out that between 295 K and T_B the dynamics does not show VFT behavior. The least-squares fit to the data from the former temperature range shown in Fig. 6 delivers the parameters $\log_{10}[\nu_0(\mathrm{Hz})] = 11.1$, $B = 753$ K, and $T_0 = 277.6$ K, in agreement with Ref. [51]. Linearizing Eq. (7) by means of differential operator $[d \log_{10} \nu / dT]^{-1/2} = (B/\ln 10)^{-1/2}(T - T_0)$ introduced by Stickel *et al.* [51], one can test in convenient way the applicability of VFT law. The bottom part of Fig. 7 shows such a plot. A linear fit to the data from above 325 K gives $B = 760$ K and $T_0 = 277.3$ K, in agreement with Fig. 6.

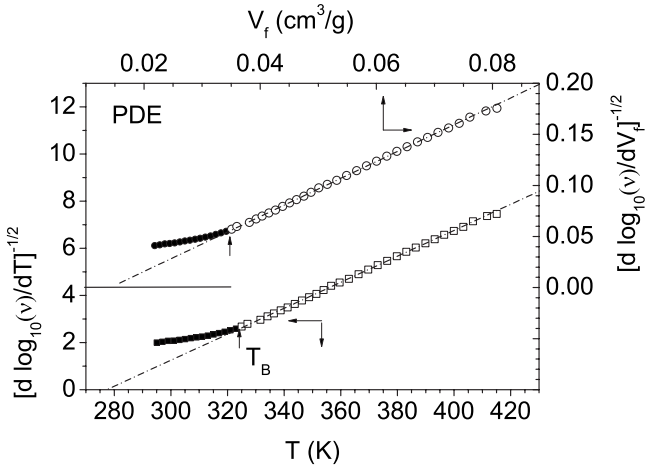

FIG. 7. Plot of $[d \log_{10}\nu / dT]^{-1/2}$ vs T (squares, bottom x and left y axes) and $[d \log_{10}\nu / dV_f]^{-1/2}$ vs V_f (circles, top x and right y axes) for PDE. The dashed-dotted lines are linear fits to the data from above $T_B = 325$ K (open symbols).

On the basis of an extension [35–39] of the CT free-volume model the structural relaxation frequency can be described by

$$\nu = C \exp[-\gamma V_f^*/(V_f - \Delta V)], \tag{8}$$

where V_f is the mean specific free volume, γV_f^* is the minimum specific free volume required for the occurrence of the process, $\gamma=0.5-1$, and ΔV is a volume correction term. In case of the full validity of the Cohen-Turnbull theory—i.e., $\Delta V=0$—the VFT law can be derived from Eq. (8), assuming a linear expansion of the free volume, $V_f=E_f(T-T_0')$ where E_f is the specific thermal expansivity and T_0' the temperature where the linearly extrapolated free volume vanishes. Comparison of Eqs. (7) and (8) leads to $\nu_0=C$, $B=\gamma V_f^*/E_f$, and $T_0=T_0'$.

Our results indicate that T_0 is larger than T_0'. This leads to a curvature in the CT plot ($\log_{10}\nu$ vs $1/V_f$) as can be observed in the top part of Fig. 7. Here we used for V_f the data calculated from $V_f=V\text{-}V_{occ}$, which do not show the "knee" behavior. This behavior can be described by Eq. (8), which corrects the free volume by the term ΔV. It was found that Eq. (8) generally describes well the segmental (α-)relaxation data of polymers and that ΔV may range from $\Delta V=0$ (low-T_g polymers with flexible chains) [35,37,39] to $\Delta V=0.06$ cm^3/g (high-T_g polymers with stiffer chains) [36]. Moreover, ΔV follows the relation $\Delta V=E_f(T_0\text{-}T_0')$. The diffusion of small molecules (gases [29–31], ions [32,33]) through polymers is generally well described by the CT free-volume theory ($\Delta V=0$).

A fit to data acquired at temperatures above $T_B=325$ K (top part of Fig. 6) delivers the parameters $\log_{10}[C(\mathrm{Hz})]=11.80(\pm0.1)$, $\gamma V_f^*=0.313(\pm0.01)$ cm^3/g, and $\Delta V=0.0138(\pm0.001)$ cm^3/g. Analogously to the VFT law, Eq. (8) can be linearized by introducing the form [37]

$$[d\log_{10}\nu/dV_f]^{-1/2} = \frac{[d\log_{10}\nu/dT]^{-1/2}}{[dV_f/dT]^{-1/2}} = \left(\frac{\gamma V_f^*}{\ln 10}\right)^{-1/2}(V_f-\Delta V). \tag{9}$$

The top part of Fig. 7 shows plots of $[d\log_{10}\nu/dV_f]^{-1/2}$ vs V_f. $[d\log_{10}\nu/dT]^{-1/2}$ was taken from the work of Stickel *et al.* [51] and $[dV_f/dT]^{-1/2}$ from our work. The data from above 325 K follow Eq. (9). A linear fit gives $\gamma V_f^*=0.317(\pm0.01)$ cm^3/g and $\Delta V=0.0142(\pm0.001)$ cm^3/g.

The findings $\Delta V>0$ may be considered as an indication that it is not the entire specific hole free volume V_f, as calculated from the PALS data, that is related to the main relaxation process via the free-volume mechanism, but a smaller portion, V_f-ΔV. In this context it is physically reasonable to assume that the lower wing of the hole size distribution contains holes too small to show a liquid like behavior and an activation energy is required for the cooperative rearranging of molecules. Larger holes may, however, show this behavior and allow a free exchange of free volume in their surroundings by thermal fluctuations—i.e. without a thermal activation in the ordinary sense. We note that the correction term ΔV is not very large, indicating that the volume governs the structural dynamics more than the thermal energy does. This behavior is typical for glass formers with small free-volume fractions [38,39].

Since the classical CT theory does not perfectly fit the structural relaxation data, we investigate in the following section whether its extension in the form of the CG free-volume model [13] provides a better description. This investigation is also stimulated by the observation by one of us [70], that the CG model seems perfectly to describe the relaxation data of PDE as well as other [71,72] glass formers over a range of 11 decades in frequency. The CG model divides the system into liquidlike and solidlike cells; only the former have a free volume large enough to be suitable for structural movements. Cohen and Grest derived that the relaxation time and the free volume vary as

$$\log_{10}\tau(T) = -\log_{10}\nu(T) = A^{CG} + B^{CG}/\{T - T_0^{CG} + [(T-T_0^{CG})^2 + C^{CG}T]^{1/2}\} \tag{10}$$

and

$$V_f(T) = B'^{CG}\{T - T_0^{CG} + [(T-T_0^{CG})^2 + C'^{CG}T]^{1/2}\}, \tag{11}$$

respectively, where $B'^{CG}\neq B^{CG}$ and $C'^{CG}\neq C^{CG}$ (for the meaning of the constants see Ref. [13]). T_0^{CG} is identified as the temperature at which continuity of the liquidlike molecules is attained (percolation threshold).

As shown by one of us [70] a fit of Eq. (10) to the dielectric relaxation times of PDE delivers the parameters $A^{CG}=-10.26$, $B^{CG}=319$, $C^{CG}=6.85$, and $T_0^{CG}=320(\pm1)$ K where τ and T are given in s and K, respectively. The fit is rather perfect ($R^2=0.9999$) over the whole range of frequencies and temperatures ($295\mathrm{K}<T<415$ K), respectively. The fitted data are plotted in the bottom part of Fig. 6 as a solid line. As discussed in Ref. [70], $T_0^{CG}=320$ K agrees with T_B, the temperature of the crossover from the VTF to another dynamics. Such a behavior was also observed for other van der Waals glass formers.

In the context of our discussion there appears the interesting question whether the excellent fit of the CG model to the dielectric structural relaxation data is of physical relevance or only the consequence of the larger variability in the fit function due to the larger number of parameters (one more than in the VFT law). We have therefore fitted the free-volume data from PVT experiments, $V_f=V\text{-}V_{occ}$, shown in Fig. 5 to Eq. (11). A fit in the temperature range between T_g and 423 K provides us following values of the parameters: $B'^{CG}=2.8\times10^{-4}$, $C'^{CG}=12.86$, and $T_0^{CG}=279(\pm1)$ K ($R^2=0.9999$), where V_f and T are given in cm^3/g and K, respectively. T_0^{CG} is 40 K lower than estimated from the relaxation data. Obviously, the CG free-volume model does not consistently describe both relaxation and free-volume data. The apparent correlation between relaxation and PALS data discussed for diethyl phthalate (DEP) by Pawlus *et al.* [72] may be attributed to the small temperature range available from the PALS data for the CG fit.

Ngai *et al.* [44] observed for "fragile" glass-forming liquids, such as ortho-terphenyl (OTP) and propylene carbonate (PC), that $T_{kv}/T_g\approx T_B/T_g\approx1.2$ while for "stronger" glasses like glycerol and propylene glycol (PG) $T_{kv}/T_g\approx T_B/T_g$

≈ 1.5 was found. An analogous behavior has been observed also by the Bratislava group [43,45,48,49]. The *o*-Ps lifetime of PDE behaves like τ_3 of the fragile glass formers OTP and PC, however with the deviation that $T_{kv}/T_g=1.23$ but $T_B/T_g=1.1$. Apparently there is no particular behavior of the mean o-Ps hole volume at T_B and no in the DS relaxation map at T_{kv}. The Bratislava group assumed in their analyses that the *o*-Ps hole volume expansion shows an intermediate transition at T_{b1} located between T_g and $T_{b2}(=T_{kv})$. Although our $\langle v_h \rangle$ data show a rather soft transition from the liquid to the glass around 300 K (Fig. 3), this behavior is well described by the parabolic fit to V_f (Fig. 5) without any extra distinct transition. We remark that the volume parameters determined here for PDE correspond well to those found for monomeric DGEBA where the dielectric relaxation shows transitions at $T_{B1}/T_g=T_\beta/T_g=1.12$ and $T_{B2}/T_g=T_\gamma/T_g=1.38$. The PALS data gave $\Delta V \approx 0$ for $T_g<T<T_{B1}$ (α relaxation) and $\Delta V=0.015$ cm^3/g for $T_{B1}/T_g<T/T_g<1.75$ (a and a' relaxation) [37].

E. Thermal fluctuations of the hole free volume and dynamic heterogeneity

The width σ_h of the hole volume distribution of the liquid mirrors the thermal volume fluctuations on a subnanometer scale as long as $T_g<T<T_{k\sigma}$. Recently, some of us [30–34] have shown that the temperature and pressure dependence of a subvolume $\langle V_{\mathrm{SV}} \rangle$, which is considered to be the volume of the smallest representative freely fluctuating subsystem, can be estimated from the *o*-Ps lifetime dispersion using a fluctuation approach [40]. The subvolume $\langle V_{\mathrm{SV}} \rangle = \xi^3$ mirrors the characteristic length of the dynamic heterogeneity, ξ, and has a similar meaning to the smallest representative mean subvolume related to structural (α) relaxations and the volume of a cooperatively rearranging region (CRR) defined by Adam and Gibbs [73]. Based on the fluctuation approach $\langle V_{\mathrm{SV}} \rangle$ may be calculated from [42–48]

$$\langle V_{\mathrm{SV}} \rangle = \xi^3 = k_B T \kappa_f^* / \delta f^2, \tag{12}$$

where $\delta f^2=\langle \delta V_f^2 \rangle / \langle V_{\mathrm{SV}} \rangle^2$ is the mean square fluctuation of the fractional free volume, $\langle V_f \rangle = (N_h' \rho) \langle V_{\mathrm{SV}} \rangle \langle v_h \rangle$ is the mean free volume within the subvolume $\langle V_{\mathrm{SV}} \rangle$, $\langle \delta V_f^2 \rangle$ is its mean-square fluctuation, and k_B is Boltzmann's constant. $\kappa_f^* = -[(1/V)(dV_f/dP)]_T$ denotes the mean fractional compressibility of the free volume, which can be approximated by $\kappa_f^* = \kappa - \kappa_{\mathrm{occ}}^*$. An estimation for $\delta f = (\delta f^2)^{1/2}$ can be obtained from

$$\delta f = (N_h' \rho) \sigma_h = N_h \sigma_h, \tag{13}$$

where $\langle \delta N_h'^2 \rangle = 0$ (taking into consideration that $N_h' = \mathrm{const}$) was assumed. Equations (12) and (13) give a lower limit of the true $\langle V_{\mathrm{SV}} \rangle$ since several holes within the same subvolume may fluctuate at a given moment in opposite directions which reduces the true value of δf [37–40].

For an estimation we assumed $\kappa_f^* \approx \kappa$ and derived the compressibility of the total volume κ from the Tait equation of PDE [10]. Between 293 K ($\approx T_g$) and 343 K, κ increases from 1.88 to 2.48 in units of 10^{-4} MPa^{-1}, while $\delta f = N_h \sigma_h$ (and $f = N_h \langle v_h \rangle$) rises from 0.014 to 0.022 (from 0.0315 to 0.0573). Correspondingly, the estimated value of $\langle V_{\mathrm{SV}} \rangle$ decreases from 4.1 nm^3 to 2.6 nm^3, as shown in Fig. 8. The length of dynamic heterogeneity, $\xi = \langle V_{\mathrm{VS}} \rangle^{1/3}$, decreases from 1.6 nm to 1.4 nm in that temperature range. This behavior corresponds qualitatively to that expected from theoretical considerations and derived from dynamic calorimetry, for example [5,6,40]. Since one hole is found within a volume of $1/N_h \approx 2.3$ nm^3, the subvolume contains ≈ 2 (or more small, $\langle v_h \rangle = 0.073$ nm^3) holes at T_g and the estimated value for $\langle V_{\mathrm{SV}} \rangle$ represents a lower limit. Further theoretical reasons for quantitative deviations between the results from PALS and dynamic calorimetry were discussed in detail in a previous paper [40]. Some of us have estimated that for polymers with flexible chains (low T_g), such as PMPS [39] and PIB [35] and also monomeric DGEBA [45] $\langle V_{\mathrm{SV}} \rangle$ varied from ≈ 8 nm^3 to 1.5–3 nm^3 when T/T_g increases from 1 to ≈ 1.2. For polymers with less flexible chains (high T_g) the calculated $\langle V_{\mathrm{SV}} \rangle$ has distinctly smaller values at T_g, which was attributed to the topologic (nonthermal) disorder in these polymers [40].

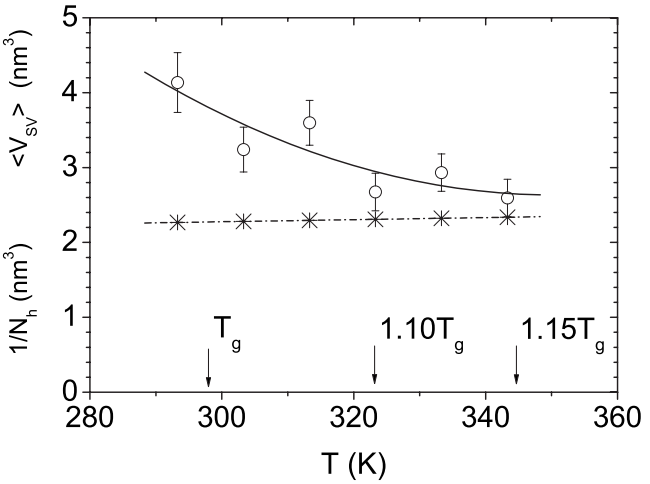

FIG. 8. Mean volume $\langle V_{\mathrm{SV}} \rangle$ (circles), considered as the volume of the smallest representative freely fluctuating subsystem, from the PALS and PVT data as a function of the temperature T at zero pressure. For comparison the volume which contains one hole, $1/N_h$ (stars), is plotted. The lines show linear and parabolic fits, respectively.

Above $T/T_g=1.10-1.15$ ($\approx T_{k\sigma}/T_g$) the subvolume $\langle V_{\mathrm{SV}} \rangle$ remains constant and corresponds to $\approx 1/N_h$; i.e., the subvolume contains just one (large, $\langle v_h \rangle = 0.14$ nm^3) hole. The subvolume may be imaged as a sphere of the (mean) diameter of 1.7 nm, which contains in the center a hole of the diameter of 0.7 nm. The hole is surrounded by a molecular shell of 0.5 nm thickness. All particles (molecules) in the neighborhood of the hole can make a jump into the hole and are, therefore, dynamically equivalent.

This picture means that at $T/T_g \approx 1.10$ the dynamic heterogeneity of the liquid disappears and the liquid transforms from a "cold" (heterogeneous) to a "hot" (homogeneous or true) liquid. In the "cold" liquid several small holes (and smaller gaps not detected by *o*-Ps) occupy the subvolume $\langle V_{\mathrm{VS}} \rangle$ and allow a cooperative rearrangement of particles. In

the "hot" liquid in the average one larger hole occupies $\langle V_{VS} \rangle$ and each neighbor particle may make a jump into the hole without massive cooperative rearrangement [37,40]. Usually, this point is also characterized by a change in the dynamics and parameters of the VFT law. For PDE this change is observed at $T_B/T_g = 1.10$.

IV. CONCLUSIONS

In the present paper, the hole free volume of the molecular glass former phenylphthalein-dimethylether (PDE) was investigated as function of temperature by PALS. The mean and standard deviation of the *o*-Ps lifetime distribution, τ_3 and σ_3, and the corresponding parameters of the volume distribution ($\langle v_h \rangle$ and σ_h) of subnanometer-size holes where *o*-Ps is localized and annihilated show a typical glass transition behavior with a weak linear expansion below $T_g = 292$ K and a strong above that temperature. The PALS T_g is in agreement with the T_g derived from PVT and dynamic experiments. At a "knee" temperature $T_k \approx 1.2 T_g$ both values show a leveling off. From plots of the specific volume V versus the hole volume $\langle v_h \rangle$ the number density of holes is estimated to be 0.32×10^{21} g^{-1}, corresponding to 0.44 nm^{-3} at room temperature. The estimated free-volume fraction f varies between $T_g = 292$ K and 423 K from $f = 0.028$ to 0.108.

It is found that the Cohen-Turnbull free-volume theory describes the structural dynamics as shown by dielectric spectroscopy only after introducing a corrected free volume $(V_f - \Delta V)$, where ΔV was estimated to be 0.014 cm^3/g. It is concluded that it is not the entire specific hole free volume V_f, as calculated from the PALS data, which is related to the main relaxation process via the free-volume mechanism, but a smaller portion. Small holes may not show a liquidlike behavior in their surroundings, and an activation energy is required for the cooperative rearranging of molecules. Larger holes may, however, show this behavior and allow a free exchange of free volume by thermal fluctuations—i.e., without a thermal activation in the ordinary sense. ΔV has a rather small value which shows that the volume governs the structural dynamics more than the thermal energy does. We found that the free-volume theory of Cohen and Grest, which has one fit parameter more than the classical Cohen-Turnbull theory, can be fitted with high accuracy to the dielectric-relaxation and free-volume data, but the parameters of both fits are not consistent. From this it follows that this free-volume theory does not describe the structural relaxation correctly.

PDE shows some features which differ from those observed for polymers. The "knee" in the hole volume expansion at $T_{kv}/T_g = 1.23$ has no correspondence in the structural dynamics and also not in the ratio between the *o*-Ps, τ_3, and structural relaxation, τ_α, lifetimes. On the other hand, as observed by dielectric spectroscopy, changes in the VFT parameters at $T_B/T_g = 1.10$ have no observable effect on the mean value of the free volume. However, the volume of the smallest representative freely fluctuating subsystem, $\langle V_{SV} \rangle$, estimated from the standard deviation of the hole size distribution σ_h, decreases between 293 K ($\approx T_g$) and 323–343 K ($T/T_g = 1.10$–1.15) from 4.1 nm^3 to 2.6 nm^3, in good agreement with polymers with flexible chains. It is concluded that at $T/T_g \approx 1.10 = T_B/T_g$ the system transforms from a heterogeneous (cold) to a homogeneous (hot) liquid.

ACKNOWLEDGMENTS

The authors would like to thank Dr. J. Kansy (Katowice) for delivering the new routine LT 9.0. We thank also Dipl. Ing. St. Rehders for help in operating the PALS apparatus. M. P. wishes to acknowledge the financial support of the Committee for Scientific Research, Poland KBN, Grant No 1P03B 075 28.

[1] G. Adam and J. H. Gibbs, J. Chem. Phys. **43**, 139 (1965).
[2] G. P. Johari and M. Goldstein, J. Chem. Phys. **53**, 2372 (1970).
[3] W. Götze and L. Sjögren, Rep. Prog. Phys. **55**, 241 (1992).
[4] M. D. Ediger, C. A. Angell, and S. R. Nagel, J. Phys. Chem. **100**, 13200 (1996).
[5] H. Sillescu, J. Non-Cryst. Solids **243**, 81 (1999).
[6] E. Donth, *The Glass Transition: Relaxation Dynamics in Liquids and Disordered Materials* (Springer, Berlin, 2001).
[7] K. L. Ngai, J. Non-Cryst. Solids **275**, 7 (2000).
[8] K. L. Ngai, in *Slow Dynamics in Complex Systema: 3rd International Symposium on Slow Dynamics in Complex Systems*, edited by Michio Tokuyama and Irwin Oppenheim, AIP Conf. Proc. No. 708 (AIP, Melville, NY, 2004), p. 515; in *Nonlinear Dielectric Phenomena in Complex Liquids*, edited by S. J. Rzoska and V. P. Shelezny NATO Science Series II, Mathematics, Physics and Chemistry (Kluwer, Dordrecht, 2004), Vol. 157, p. 247.
[9] A. Patkowski, M. Paluch, and H. Kriegs, J. Chem. Phys. **117**, 2192 (2002).
[10] M. Paluch, R. Casalini, A. Bests, and A. Patkowski, J. Chem. Phys. **117**, 7624 (2002).
[11] M. Paluch, R. Casalini, and C. M. Roland, Phys. Rev. B **66**, 092202 (2002).
[12] M. H. Cohen and D. Turnbull, J. Chem. Phys. **31**, 1164 (1959); D. Turnbull and M. H. Cohen, *ibid.* **52**, 3038 (1970).
[13] G. S. Grest and M. H. Cohen, Adv. Chem. Phys. **48**, 455 (1981).
[14] C. Sharma, editor, *Positron Annihilation Studies of Fluids* (Wold Scientific, Singapore, 1988).
[15] O. E. Mogensen, *Positron Annihilation in Chemistry* (Springer, Berlin, 1995).
[16] R. A. Pethrick, Prog. Polym. Sci. **22**, 1 (1997); B. D. Malhotra and R. A. Pethrick, Phys. Rev. B **28**, 1256 (1983).
[17] *Principles and Application of Positron and Positronium Chemistry*, edited by Y. C. Jean, P. E. Mallon, and D. M. Schrader, (World Scientific, Singapore, 2003).
[18] J. Bartoš, in *Encyclopedia of Analytical Chemistry*, edited by R. A. Meyers (Wiley, Chichester, 2000), p. 7968.
[19] F. Faupel, J. Kanzow, K. Günther-Schade, C. Nagel, P. Sperr, and G. Kögel, in *Positron Annihilation, Proceedings of the 13th International Conference (ICPA-13)*, edited by T. Hyodo,

Y. Kobayashi, Y. Nagashima, and H. Saito [Mater. Sci. Forum 445–446, 219 (2004)].
[20] Y. C. Jean, Macromolecules **29**, 5756 (1996).
[21] A. H. Baugher, W. J. Kossler, and K. G. Petzinger, Macromolecules **29**, 7280 (1996).
[22] S. J. Tao, J. Chem. Phys. **56**, 5499 (1972).
[23] M. Eldrup, D. Lightbody, and J. N. Sherwood, Chem. Phys. **63**, 51 (1981).
[24] H. Nakanishi, S. J. Wang, and Y. C. Jean, in *Positron Annihilation Studies of Fluids*, edited by S. C. Sharma (Wold Scientific, Singapore, 1988), p. 292.
[25] R. B. Gregory, J. Appl. Phys. **70**, 4665 (1991).
[26] Q. Deng, F. Zandiehnadem, and Y. C. Jean, Macromolecules **25**, 1090 (1992).
[27] G. Dlubek, J. Stejny, and M. A. Alam, Macromolecules **31**, 4574 (1998).
[28] R. Srithawatpong, Z. L. Peng, B. G. Olson, A. M. Jamieson, R. Simha, J. D. McGervey, T. R. Maier, A. F. Halasa, and H. Ishida, Ber. Bunsenges. Phys. Chem. **37**, 2754 (1999).
[29] C. Nagel, K. Günther-Schade, D. Fritsch, T. Strunskus, and F. Faupel, Macromolecules **35**, 2071 (2002).
[30] C. Nagel, E. Schmidtke, K. Günther-Schade, D. Hofmann, D. Fritsch, T. Strunskus, and F. Faupel, Macromolecules **33**, 2242 (2000).
[31] J. Kruse, J. Kanzow, K. Rätzke, F. Faupel, M. Heuchel, J. Frahn, and D. Hofmann, Macromolecules **38**, 9638 (2005).
[32] G. Dlubek, D. Kilburn, and M. A. Alam, Electrochim. Acta **49**, 5241 (2004); **50**, 2351 (2005).
[33] D. Bamford, A. Reiche, G. Dlubek, F. Alloin, J.-Y. Sanchez, and M. A. Alam, J. Chem. Phys. **118**, 9420 (2003).
[34] G. Dlubek, A. Sen Gupta, J. Pionteck, R. Krause-Rehberg, H. Kaspar, and K. H. Lochhaas, Macromolecules **37**, 6606 (2004).
[35] D. Kilburn, J. Wawryszczuk, G. Dlubek, J. Pionteck, R. Häßler, and M. A. Alam, Macromol. Chem. Phys. **207**, 721 (2006).
[36] D. Kilburn, G. Dlubek, J. Pionteck, and M. A. Alam, Polymer **47**, 7774 (2006).
[37] G. Dlubek, E. M. Hassan, R. Krause-Rehberg, and J. Pionteck, Phys. Rev. E **73**, 031803 (2006).
[38] G. Dlubek, J. Pionteck, M. Q. Shaikh, E. M. Hassan, and R. Krause-Rehberg, Phys. Rev. E **75**, 021802 (2007).
[39] G. Dlubek, M. Q. Shaikh, R. Krause-Rehberg, and M. Paluch, J. Chem. Phys. **126**, 024906 (2007).
[40] G. Dlubek, J. Non-Cryst. Solids **352**, 2869 (2006).
[41] J. Bartoš and J. Krištiak, J. Non-Cryst. Solids **235-237**, 293 (1998).
[42] Sz. Vass, A. Patkowski, E. W. Fischer, K. Süvegh, and A. Vértes, Europhys. Lett. **46**, 815 (1999).
[43] J. Bartoš and J. Krištiak, J. Phys. Chem. B **104**, 5666 (2000).
[44] K. L. Ngai, L.-R. Bao, A. F. Yee, and Ch. L. Soles, Phys. Rev. Lett. **87**, 215901 (2001).
[45] J. Bartoš, O. Šauša, J. Krištiak, T. Blochowicz, and E. Rössler, J. Phys.: Condens. Matter **13**, 11473 (2001); J. Bartoš, O. Šauša, D. Račko, J. Krištiak, and J. J. Fontanella, J. Non-Cryst. Solids **351**, 2599 (2005).
[46] J. T. Bendler, J. J. Fontanella, M. F. Shlesinger, J. Bartoš, O. Šauša, and J. Krištiak, Phys. Rev. E **71**, 031508 (2005).
[47] D. Račko, R. Chelli, G. Cardini, J. Bartoš, and S. Califano, Eur. Phys. J. D **32**, 289 (2005).
[48] S. Pawlus, J. Bartoš, O. Šauša, J. Krištiak, and M. Paluch, J. Chem. Phys. **124**, 104505 (2006).
[49] J. Bartoš, A. Alegria, O. Šauša, M. Tyagi, D. Gómez, J. Krištiak, and J. Colmenero, Phys. Rev. E **76**, 031503 (2007).
[50] J. Kansy, Nucl. Instrum. Methods Phys. Res. A **374**, 235 (1996); J. Kansy, LT for Windows, Version 9.0, Institute of Physical Chemistry of Metals, Silesian University, Bankowa 12, PL-40–007 Katowice, Poland, 2002 (private communication).
[51] F. Stickel, E. W. Fischer, and R. Richert, J. Chem. Phys. **104**, 2043 (1996).
[52] P. Kirkegaard, N. J. Pederson, and M. Eldrup, computer code PATFIT-88, Tech. Rep. Risø-M-2740, Risø National Laboratory, DK-4000 Roskilde, Denmark, 1989.
[53] S. V. Stepanov and V. M. Byakov, in *Principles and Application of Positron and Positronium Chemistry*, edited by Y. C. Jean, P. E. Mallon, and E. M. Schrader (World Scientific, Singapore, 2003), p. 117.
[54] M. Rudel, J. Kruse, K. Rätzke, F. Faupel, Yu. P. Yampolskii, V. P. Shantarovich, and G. Dlubek, Macromolecules **41**, 788 (2008).
[55] M. Eldrup, in *Positron Annihilation*, edited by P. G. Coleman, S. C. Sharam, and L. M. Daina (North-Holland, Amsterdam, 1982), p. 753.
[56] G. Dlubek, A. Sen Gupta, J. Pionteck, R. Häßler, R. Krause-Rehberg, H. Kaspar, and K. H. Lochhaas, Polymer **46**, 6075 (2005).
[57] J. Liu, Q. Deng, and Y. C. Jean, Macromolecules **26**, 7149 (1993).
[58] T. Kanaya, I. Tsukushi, K. Kaji, J. Bartoš, and J. Krištiak, Phys. Rev. E **60**, 1906 (1999).
[59] S. Kahle, J. Gapinski, G. Hinze, A. Patkowski, and G. Meier, J. Chem. Phys. **122**, 074506 (2005).
[60] R. Simha and T. Somcynsky, Macromolecules **2**, 342 (1969).
[61] R. E. Robertson, in *Computational Modelling of Polymers*, edited by J. Bicerano (Marcel Dekker, Midland, MI, 1992), p. 297.
[62] L. A. Utracki and R. Simha, Macromol. Theory Simul. **10**, 17 (2001).
[63] Z. Yu, U. Yahsi, J. D. McGervey, A. M. Jamieson, and R. Simha, Ber. Bunsenges. Phys. Chem. **32**, 2637 (1994).
[64] M. Schmidt and F. H. J. Maurer, Macromolecules **33**, 3879 (2000).
[65] G. Consolati, F. Quasso, R. Simha, and B. G. Olson, Ber. Bunsenges. Phys. Chem. **43**, 2225 (2005).
[66] G. Consolati, J. Phys. Chem. B **109**, 10096 (2005).
[67] G. Dlubek, J. Pionteck, and D. Kilburn, Macromol. Chem. Phys. **205**, 500 (2004).
[68] D. Kilburn, G. Dlubek, J. Pionteck, D. Bamford, and M. A. Alam, Polymer **46**, 859 (2005); **46**, 869 (2005).
[69] R. Simha and U. Yashi, J. Chem. Soc., Faraday Trans. **91**, 2443 (1995).
[70] M. Paluch, R. Casalini, and C. M. Roland, Phys. Rev. E **67**, 021508 (2003).
[71] U. Schneider, P. Lunkenheimer, R. Brand, and A. Loidl, Phys. Rev. E **59**, 6924 (1999).
[72] S. Pawlus, J. Bartos, O. Sausa, J. Kristiak, and M. Paluch, J. Chem. Phys. **124**, 104505 (2006).
[73] G. Adam and J. H. Gibbs, J. Chem. Phys. **43**, 139 (1965).